Communication

The role of actin and microtubule networks in plasmid DNA intracellular trafficking

Vladan Ondřej✉, Emilie Lukášová, Martin Falk and Stanislav Kozubek

Laboratory of Molecular Cytology and Cytometry, Institute of Biophysics, Academy of Sciences of the Czech Republic, Brno, Czech Republic

This work is focused on the function of the microtubule and actin networks in plasmid DNA transport during liposomal transfection. We observed strong binding of plasmid DNA–lipid complexes (lipoplexes) to both networks and directional long-range motion of these lipoplexes along the microtubules. Disruption of either of these networks led to the cessation of plasmid transport to the nucleus, a decreased mobility of plasmids, and accumulation of plasmid DNA in large aggregates at the cell periphery. Our findings show an indispensable but different role of both types of cytoskeleton, actin and microtubular, in the processes of gene delivery.

INTRODUCTION

The intracellular transport of plasmid DNA, in the context of gene delivery by transfection using non-viral vectors, is still poorly explored. Relatively little is known about the kinetics and fate of the transfected DNA, such as its intracellular transfer and localization. A variety of intracellular barriers must be overcome to deliver exogenous DNA into the cell nucleus of the host cell to allow its expression. Vectors must cross the plasma membrane, move through the cytoplasm, enter the nucleus, and then locate to a specific site suitable for vector integration and DNA transcription. The intracellular movement of plasmid DNA complexes affecting gene delivery may represent one of the major barriers, and remains to be explored (Zhou *et al.*, 2004). Many authors found that plasmid DNA entered the cells within 1 h after transfection, and that this DNA accumulated in the perinuclear region (Zabner *et al.*, 1995; Coonrod *et al.*, 1997; Johnson & Jurcisek, 1999). It has also been shown by Lukacs *et al.* (2000) that molecules of DNA larger than 2000 bp are unable to diffuse freely in the cytoplasm. However, it is known that despite this apparent inability of plasmids to diffuse through the cytoplasm, transfections do result in expression. Thus, plasmids must be able to cross the cytoplasm by other means than diffusion.

Trafficking of viral DNA has been studied more intensively. Like plasmids, viruses enter their hosts and traverse the cytoplasm to enter the cell nucleus for replication. Recent studies have pointed to the use by viruses of the cytoskeleton to facilitate transport towards the nucleus (van Loo *et al.*, 2001; McDonald *et al.*, 2002; Lee *et al.*, 2006). Viruses such as herpes simplex virus type 1 and adenovirus move to the nucleus by latching on to dynein motor proteins and moving along the microtubules (reviewed in Campbell & Hope, 2005). Recent data indicate that HIV-1 also uses dynein motors and the microtubules for its movement (reviewed in Anderson & Hope, 2005). Although microtubules appear to be the dominant highways for viruses, they are by no means the exclusive route. Van Loo *et al.* (2001) showed that baculovirus uses the actin cytoskeletal network to move towards the nucleus, using myosin V motors. Also, some mRNAs are actively translo-

✉**Corresponding author**: Vladan Ondřej, Laboratory of Molecular Cytology and Cytometry, Institute of Biophysics, Academy of Sciences of the Czech Republic, v.v.i., Královopolská 135, Brno 612 65, Czech Republic; tel.: (420) 541 517 165, fax: (420) 541 211 293, e-mail: ondrej@ibp.cz

cated from nuclear pores on cytoskeletal filaments, and ultimately localize at specific regions of the cell (Shav-Tal & Singer, 2005).

Like that of viruses, the transport of plasmids to the cell nucleus could also be facilitated by the cytoskeletal network. A recent contribution of Vaughan and Dean (2006) showed that disruption of microtubules or dynein inhibition decreased expression of microinjected plasmids. Taken together, these results led to the idea that plasmids probably become attached to cytoskeletal motors, much like viruses do, and move along the microtubules to the cell nucleus. Here, we report experiments with fluorescently labeled plasmid DNA transfected by means of liposomes to find and distinguish the roles of two cytoskeletal networks, actin and microtubules, in plasmid DNA trafficking throughout the cytoplasm. Labelled plasmids, together with networks visualized by means of fluorescent fusion proteins or live staining, enable us to track plasmid DNA *in vivo* and to assign dynamic parameters to it. We also followed cytoplasmic transport of plasmid DNA after network disruption using different drug treatments. Based on a series of *in vivo* cell measurements and observations of fixed cells, we conclude that the microtubule network is utilized by plasmid DNA–lipid complexes (lipoplexes) for long-range movement. Unlike complexes attached to the microtubule network, complexes attached to the actin network are highly immobile. Interestingly, disruption of either network stopped the transport of plasmid DNA and resulted in accumulation of lipoplexes at the cytoplasmic periphery.

MATERIALS AND METHODS

Cell culture and cell transfection. Fibroblasts (04-147), originated from Academic Medical Center University of Amsterdam (The Netherlands), were grown in DMEM medium, supplemented with 10% fetal calf serum (FCS), penicillin (100 U/ml) and streptomycin (100 μg/ml), in humidified air with 5% CO_2 at 37°C. Transfection was performed using Lipofectamine 2000 (Invitrogen) in OPTIMEM medium (Gibco), according to the manufacturer's protocol, in six-well multidishes or in special chambers for *in vivo* observations. After 5 h of cell transfection in the presence of Lipofectamine 2000, the medium was replaced with DMEM containing 10% FCS without antibiotics, and cells were incubated for 24 h. Before fixation, the DMEM medium was replaced with OPTIMEM to which green Lumio reagent was added to produce the recommended concentration of 2.5 μM. The cells were incubated for 30 min and then fixed or used for *in vivo* observation. To visualize microtubules *in vivo* in transfected cells, the fibroblasts were incubated with OPTIMEM medium supplemented with an appropriate volume of TubulinTracker Green (Invitrogen) for 20 min, according to the manufacturer's protocol. After that, the medium was supplemented with 200 μM trolox (Sigma-Aldrich), and the cells were ready for observation *in vivo*.

Vectors used and DNA labelling. The Lumio technology (Invitrogen) and the HORF clone of the β-actin gene (IOH3654, Invitrogen) were used for fusion protein preparation, where the fluorescent tag is a Lumio tetracysteine sequence.

The plasmid DNA, composed of the pENTR 221 vector containing β-actin cDNA, the gene for kanamycin resistance, the Kozak consensus sequence and the pUC origin, was labelled before transfection with Label IT Tracker reagent Cy5 (Mirus Co.), at the Cy5:DNA ratio recommended by the manufacturer, at 37°C for 1 h. The unbound Cy5 reagent was removed through DNA precipitation.

Drug treatment. Fibroblast cultures were treated with two different inhibitors of actin polymerization, latrunculin B (20 μM) or cytochalasin D (4 μM) (both from Sigma-Aldrich), or twice with nocodazole (20 μM) (Sigma-Aldrich) to inhibit tubulin polymerization. The first treatment was carried out 2 h after transfection, and the second one just before cell fixation. Inhibition of actin polymerization lasted 1 h, and inhibition of tubulin polymerization 2 h.

Cell fixation and immunostaining. Cells were fixed in 4% paraformaldehyde and permeabilized. The primary antibody used was mouse anti-tubulin α (Santa Cruz Biotechnology, Inc.), diluted in 7% FCS + 2% BSA/PBS. The secondary antibody was affinity-purified donkey anti-mouse-FITC-conjugated from Jackson ImmunoResearch (West Grove, PA, USA). Actin filaments were stained with rhodamine-phalloidin (Invitrogen) after tubulin detection. After brief washing in 2 × SSC, Vectashield medium (Vector Laboratories) was used for final mounting of samples. Nuclei were stained with TOPRO-3 (Molecular Probes).

Image acquisition and analysis of experimental data. For image acquisition we used an automated Leica DM RXA fluorescence microscope equipped with a CSU10a Nipkow disc (Yokogawa, Japan) for confocal imaging, a CoolSnap HQ CCD-camera (Photometrix) or alternatively an iXon DV 887ECS-BV (Andor) for *in vivo* observation, and an Ar/Kr laser (Inova 70C, Coherent), driven by a personal computer. Automated exposure, image quality control and other procedures were performed using FISH 2.0 software (Kozubek *et al.*, 2001), and the Acquiarium software was used for live cell imaging. An oil immersion Plan Fluotar objective (100×/NA 1.3) was used. Fourty optical sections (15 for live cells) at 0.3 μm steps along the z-axis were acquired for each

nucleus at a constant temperature of 26°C (37°C for live cells), and stored in the computer memory.

Changes in positions of the fluorescence signals (object tracking) were determined using the FISH 2.0 and 3D viewer software (Kozubek *et al.*, 2004), which allowed us to assign 3D coordinates to the fluorescence signals. The coordinates were taken at the centre of gravity of the visualized objects. The subsequent images of lipoplexes were captured every 30 s for 1 min. The lipoplexes were traced in the time-lapse series on the basis of matching algorithms (Kozubek *et al.*, 2004). In 3D, the length of the lipoplex trajectory was calculated using the equation: $d = \sqrt{(x_1-x_n)^2 + (y_1-y_n)^2 + (z_1-z_n)^2}$, where x_1, y_1 and z_1 (x_n, y_n and z_n) were coordinates for the first measurement and the n-th measurement of the same object. The mean square of differences in the length of the trajectory (Δd^2) at each time point (t) was calculated as $\Delta d^2 = (d_t - d_{t+\Delta t})^2$, where Δt was the time interval between measurements. The diffusion coefficient (D) was calculated as $D = \Delta d^2/t$. Evaluation of data, distance calculation and statistical analyses were performed using the Sigma Plot statistical package (Jandel Scientific).

RESULTS

Cytoplasmic trafficking of plasmid DNA

To investigate the role of the actin network in plasmid DNA trafficking, human fibroblasts were firstly transfected with a β-actin-Lumio construct, and plasmid DNA was then labelled with Cy5. The prepared construct bears the gene for human non-muscle β-actin protein fused with the tetracysteine Lumio tag, allowing visualisation of the fusion protein using the green Lumio reagent. Twenty-four hours after transfection, β-actin-Lumio proteins formed cytoplasmic filaments, a perinuclear actin layer, and intranuclear structures (Fig. 1). The proper formation of cytoplasmic filaments by the actin-

lumio protein was verified using phalloidin staining on fixed specimens (Fig. 1C). The microtubule network was labelled by taxol conjugated with green fluorescent dye for *in vivo* experiments.

The *in vivo* observations showed that plasmid DNA–lipid complexes were frequently bound to microtubules and actin filaments (Fig. 2). During a one-minute interval, three images were acquired and movements of the plasmid signals were analysed. Lipoplexes attached to actin filaments were highly restricted in their motion ($D = 1.42 \times 10^{-3}$ $\mu m^2/s$, number of measured lipoplexes was 17, std. error $= 5.09 \times 10^{-4}$). The average velocity (v) of the lipoplexes bound to the actin network was calculated as $v = 0.292$ µm/min (number of measured lipoplexes = 17, std. error $= 4.5 \times 10^{-2}$), which is at the lower limit of CCD camera resolution. On the other hand, lipoplexes attached to the microtubule network displayed directional motion mostly toward the cell nucleus along the microtubules, as demonstrated in representative time-lapse images (Fig. 2, bottom row of images). The average velocity along the microtubules was $v = 1.119$ µm/min (number of measured lipoplexes = 30, std. error $= 8.8 \times 10^{-2}$).

Immunostaining of microtubules and phalloidin staining of actin filaments in fixed cells transfected with labelled plasmid DNA were used to determine the location of plasmid DNA signals inside the cytoplasm in relation to both networks visualized simultaneously in the same cells. Plasmids in lipoplexes clearly bound to both networks (Fig. 3A). In many cases, plasmid signals co-localized simultaneously with the actin filament and with microtubules (Fig. 3A). The lipoplexes entered the cytoplasm by endocytosis and bound to the peripheral actin filaments. At these sites, they subsequently formed small lipoplexes, as observed in live cells (Fig. 3B). These lipoplexes were bound to both actin filaments and to microtubules (Fig. 3A). Plasmids accumulated around the nucleus, co-localized with the perinuclear actin shell, and entered the nucleus (Fig. 3C).
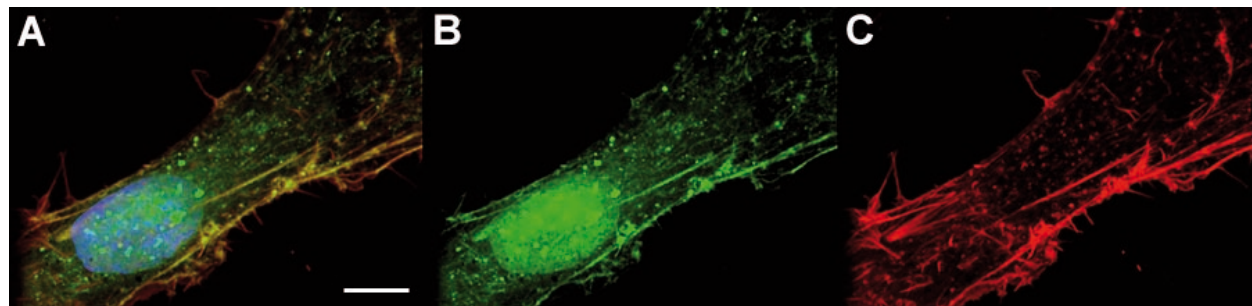
Figure 1. The actin-Lumio fusion protein expression and visualization in fibroblasts.
A fibroblast transfected with the vector bearing gene coding for the actin-Lumio fusion protein (A). The actin-Lumio protein formed cytoplasmic actin filaments visualized in green (B), which strongly co-localized with phalloidin, stained red (C). The cell nucleus visualized with TOPRO-3 (A), coincides with the distribution of nuclear actin (B). Scale bar 5 µm.
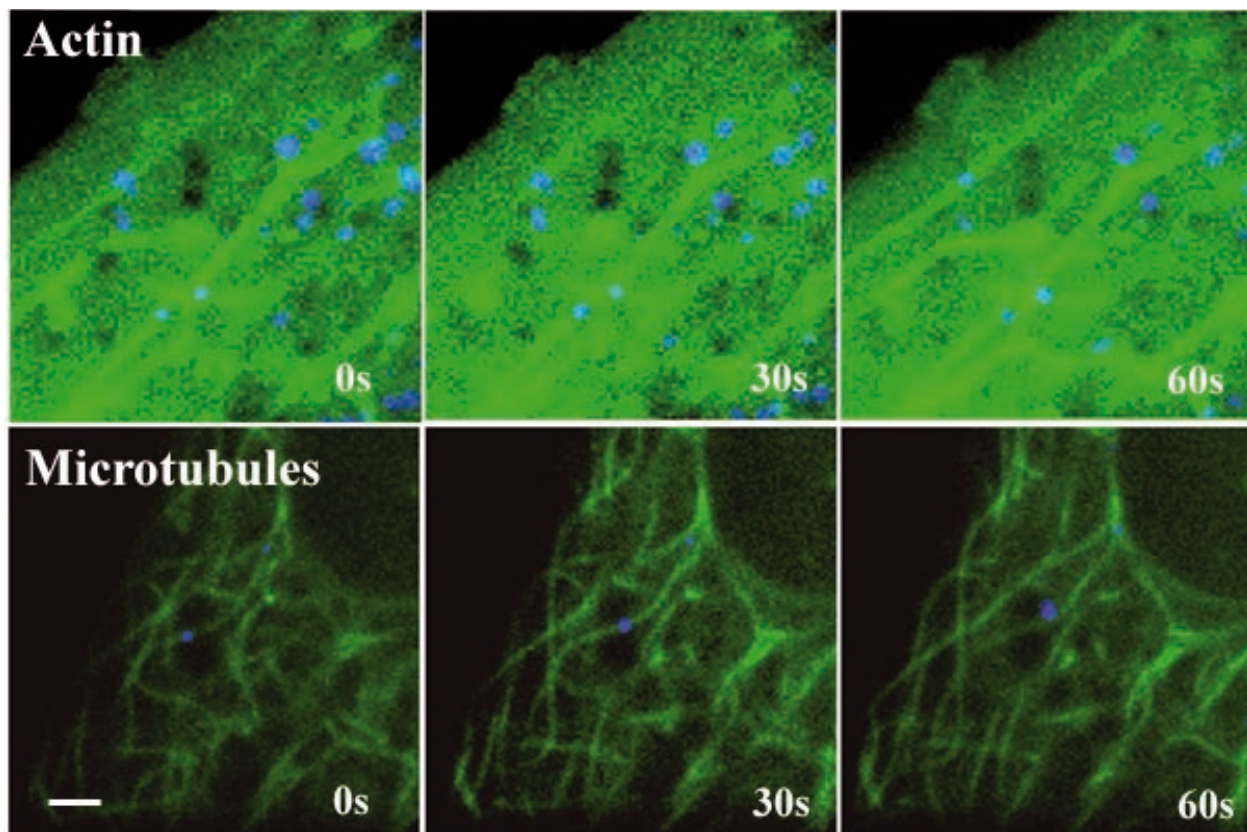
Figure 2. Movement of plasmid DNA lipoplexes in live cells visualized simultaneously with cytoskeletal networks.
The upper row of images taken at successive time points shows the highly constrained motion of lipoplexes (blue) bound to actin filaments (green), visualized by means of the actin-Lumio fusion protein. The bottom row of images demonstrates the directional movement of two lipoplexes (blue) along a microtubule towards the cell nucleus during 1 min. Scale bar 1 μm.

The role of disruption of the cytoplasmic networks in plasmid trafficking

To elucidate the role of the cytoskeleton in the trafficking of plasmids to the cell nucleus, inhibitors of polymerization of actin or microtubule networks were used (Fig. 4). Nocodazole treatment changed the shape of cells (Fig. 4A) and disrupted the microtubule network as visualized by tubulin immunostaining (Fig. 4E). The plasmid DNA lipoplexes changed their cytoplasmic location. Unlike in untreated control cells (Fig. 4H), lipoplexes accumulated in large aggregates at the cytoplasmic periphery (Fig. 4E). The lipoplexes also changed their mobility. Directional movement was not detectable, and the diffusion coefficient was similar to the value measured for the dynamics of plasmids bound to actin filaments in untreated cells (1.36×10^{-3} μm^2/s; number of measured lipoplexes = 20, std. error = 2.9×10^{-4}). The nocodazole treatment also halted plasmid transport into the cell nucleus. As Fig. 5 shows, the number of plasmid signals inside the nucleus decreased significantly compared with the number of plasmid signals in nuclei of untreated cells. Al-

though the microtubule network in nocodazole-treated cells was disrupted, the actin filaments were still visible (Fig. 4E). But this single network did not allow plasmid DNA transport.

The actin network was disrupted using treatment of cells with latrunculin B or cytochalasin D. Both drugs reversibly inhibited polymerization of actin filaments. The inhibitors disorganized the actin cytoskeleton and changed the shape of cells and nuclei (Figs. 4B, C). The inhibition of actin polymerization also changed the distribution of lipoplexes in the cytoplasm, and their mobility decreased to 3.8×10^{-4} μm^2/s (number of measured lipoplexes = 10, std. error = 1.4×10^{-4}). The plasmid DNA accumulated in large aggregates at the cytoplasmic periphery, and plasmid transport to the cell nucleus was stopped as in the case of nocodazole treatment (Figs. 4F, G). Although the microtubule network was not substantially affected by inhibitors of actin polymerization, and microtubules were visible using immunostaining of tubulin (Figs. 4F, G), there was no transport along microtubules. Disruption of plasmid transport after the treatment of cells with both types of inhibitors was also reflected in the low number of plasmid
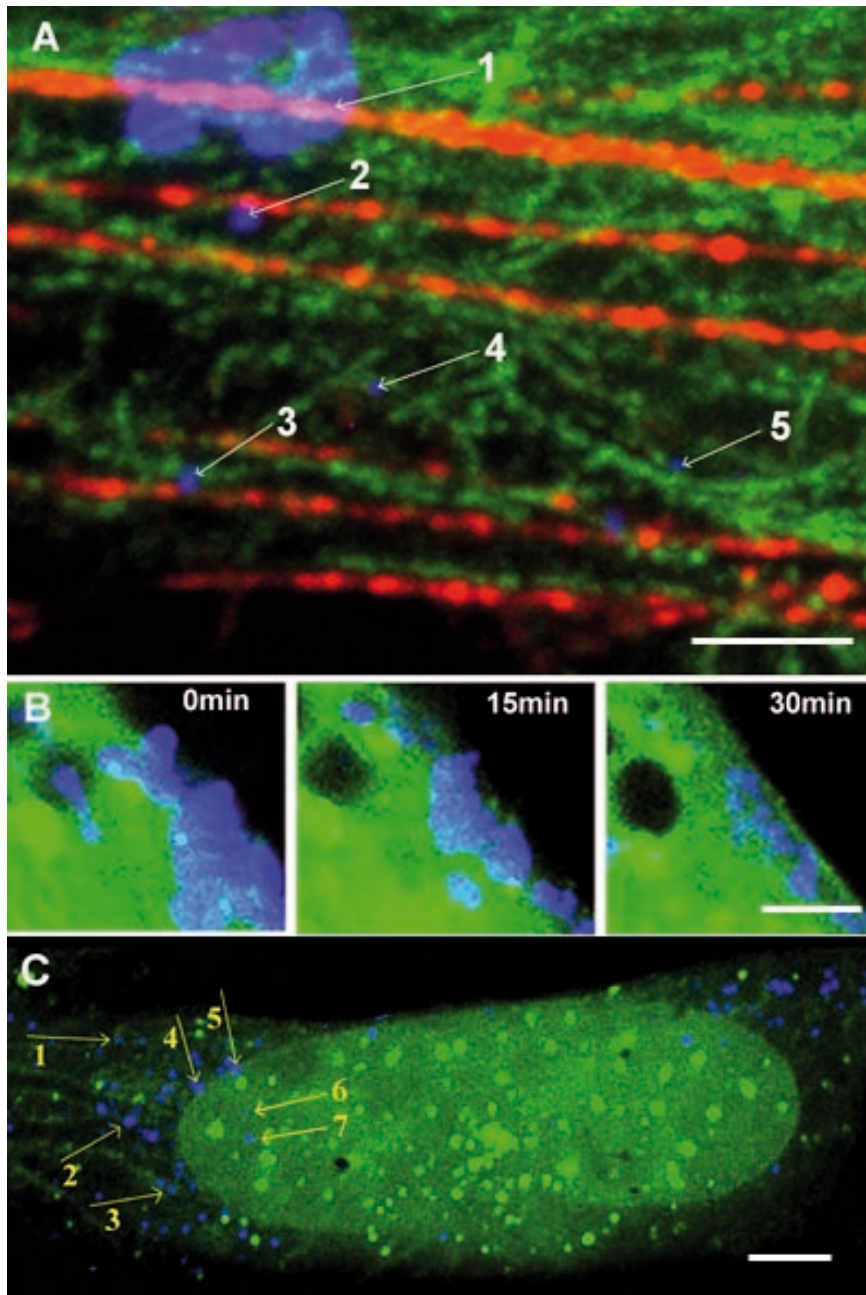
Figure 3. Distribution of lipoplexes throughout the cell cytoplasm and their binding to cytoskeletal networks.

Panel A of the image demonstrates the co-localization of signals of plasmid DNA lipoplexes (blue) with the networks inside the cytoplasm. Arrow 1 indicates a large mass of lipoplexes bound to a peripheral actin filament (red). Arrow 2 shows lipoplexes attached to the actin network (red). Arrow 3 indicates lipoplexes bound to both a microtubule (green) and an actin filament (red); arrows 4 and 5 show lipoplexes bound to microtubules only. The decomposition of the large mass of lipoplexes to the smaller ones at the periphery of the live cell is shown in panels B. The distribution of plasmid DNA lipoplexes in a whole fibroblast expressing actin-Lumio fusion protein (green) is demonstrated in panel C. The actin-Lumio proteins visualize actin filaments and the cell nucleus. Plasmid DNA is concentrated near the nucleus (yellow arrows 1–3), at the actin perinuclear shell (yellow arrows 4 and 5) and within the nucleus (yellow arrows 6 and 7). Scale bars 2 μm.

particles entering the nucleus (Fig. 4I). The results show that plasmids require both networks to be unaffected for transport towards the cell nucleus.

DISCUSSION

The purpose of this study was to analyse the roles of the cytoplasmic actin and microtubule networks in plasmid DNA trafficking. Labelled plasmid DNA was transfected into fibroblasts that expressed the fluorescent fusion protein actin-Lumio, or into fibroblasts stained with a fluorescent dye that bound to the microtubules. Using this approach, we were able to track plasmid DNA simultaneously with the cytoskeleton *in vivo*, and study the mobility of the plasmid DNA–lipid complexes in relation to the networks and its binding to them.

When plasmids enter the cell (in this work by means of liposome transfection), they need to travel long distances through the cytoplasm to reach the cell nucleus. On the other hand, Lukacs *et al.* (2000) and Dauty and Verkman (2005) have shown that DNA fragments cannot move *via* diffusion through the cytoplasm. Since diffusion through the dense meshwork of the cytoplasm is not likely, other mechanisms must exist by which plasmids can move towards the cell nucleus. Recently, it became clear that the cytoskeleton does not constitute a barrier for successful gene delivery, but on the contrary, some
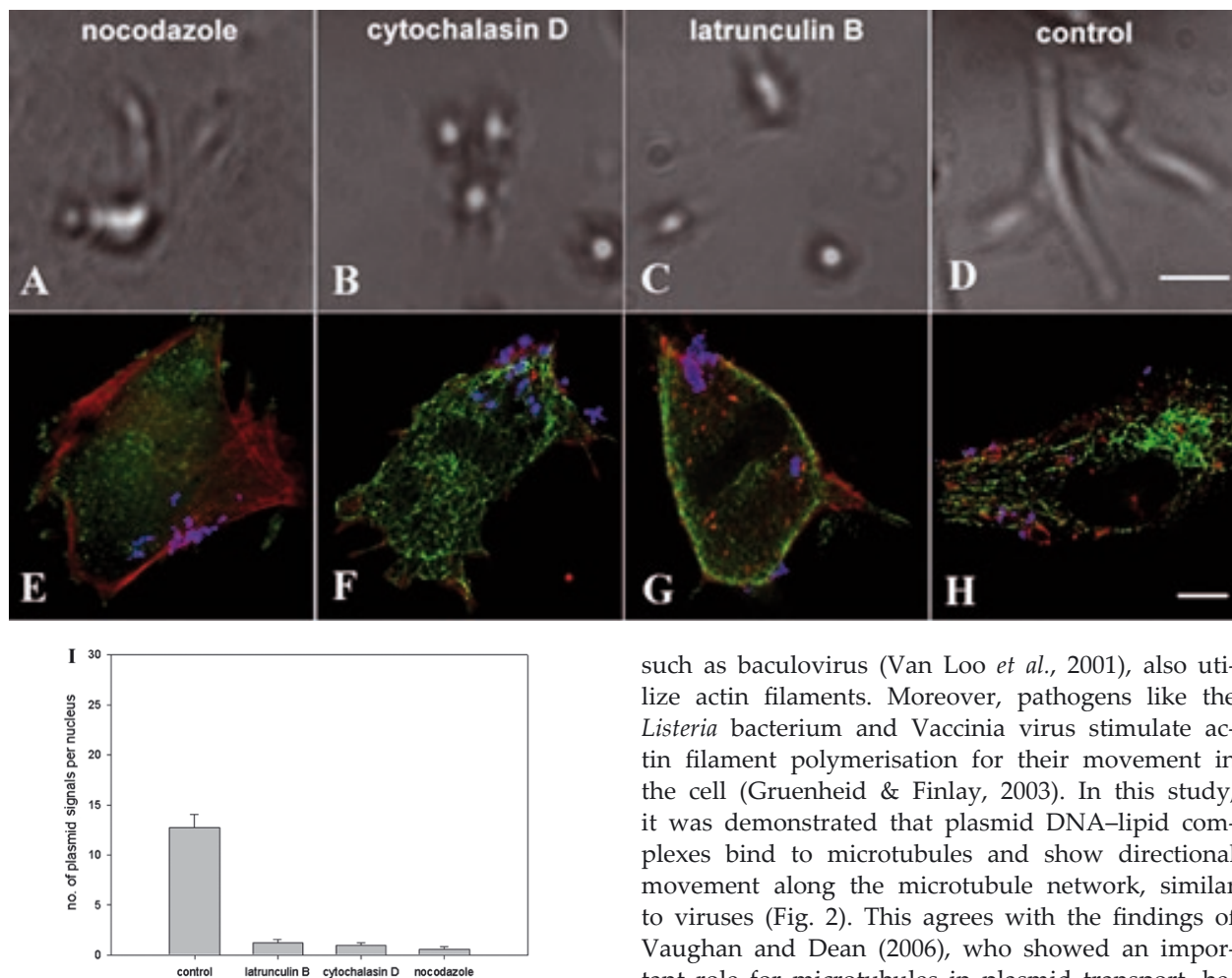
Figure 4. Disruption of cytoskeletal networks influenced the transport of lipoplexes throughout the cell cytoplasm.

Images of fibroblasts after inhibition of tubulin polymerization by nocodazole (A, E), or inhibition of actin polymerization using cytochalasin D (B, F) or latrunculin B (C, G). Nocodazole disrupted the microtubular network (green), but did not affect the actin network. Cytochalasin D and latrunculin B disrupted the actin network (red). Both types of inhibitors changed the shape of the cells, and caused accumulation of plasmid DNA lipoplexes (blue) as huge aggregates at the periphery of the cytoplasm, unlike in control cells (D, H), where signals of small lipoplexes were bound to the cytoskeleton. Scale bars 20 μm (A–D) and 5 μm (E–H). The bar graph (I) shows the decreased number of plasmid DNA signals per nucleus after treatment with the actin polymerization inhibitors, latrunculin B and cytochalasin D, or with the tubulin polymerization inhibitor nocodazole, 24 h after cell transfection.

components of cytoplasmic networks actively contribute to transport of plasmids in complexes, just as they do for viruses (Zhou *et al.*, 2004; Vaughan & Dean, 2006). As already published (McDonald *et al.*, 2002; Lee *et al.*, 2006), viruses utilize dynein motors to move along the microtubules. Some viruses,

such as baculovirus (Van Loo *et al.*, 2001), also utilize actin filaments. Moreover, pathogens like the *Listeria* bacterium and Vaccinia virus stimulate actin filament polymerisation for their movement in the cell (Gruenheid & Finlay, 2003). In this study, it was demonstrated that plasmid DNA–lipid complexes bind to microtubules and show directional movement along the microtubule network, similar to viruses (Fig. 2). This agrees with the findings of Vaughan and Dean (2006), who showed an important role for microtubules in plasmid transport, because of the decrease in expression of microinjected plasmids after the inhibition of dynein motors or disruption of microtubules. On the other hand, our results show that actin filaments immobilized the bound plasmid DNA lipoplexes. They displayed highly restricted diffusive motion, with corresponding slow randomly-oriented movement (average velocity 0.292 μm/min).

Considering these results, it was rather surprising that disruption of either of the networks investigated led to a complete stoppage of plasmid transport. Nocodazole treatment disintegrated microtubules, which inhibited plasmid trafficking, as also observed by Vaughan and Dean (2006). In our experiments, untreated cells showed accumulation of small clumps of lipoplexes at the perinuclear region, similar to the studies of Zabner *et al.* (1995) and Coonrod *et al.* (1997). After the nocodazole treatment, lipoplexes formed large aggregates at the cell periphery. This shows that plasmid transport was interrupted after the lipoplexes entered the cell, and their inability to move toward the nucleus led to their accumulation. A similar disruption of plasmid transport was achieved using inhibitors of actin polymerization, although the microtubules were not

disorganized. Although actin filaments restricted the movement of lipoplexes, it is evident that they must play some important role in plasmid trafficking. A large number of lipoplexes were localized on actin filaments and microtubules together. These results indicate that the plasmids in the complex with lipids that entered the cytoplasm first encounter the peripheral actin cytoskeleton. They become immobilized and their aggregates form smaller ones, which are probably moved to nearby microtubules and uploaded on to them as cargo. After that, the lipoplexes move towards the cell nucleus. Similarly, the actin cytoskeleton may act as a barrier to incoming retroviral vectors at the plasma membrane. However, some studies indicate that the actin network may also play a positive role in early retroviral trafficking (reviewed in Anderson & Hope, 2005; Campbell & Hope, 2005). Interestingly, the diffusion coefficient and velocity of plasmid DNA lipoplexes bound to actin filaments in the cytoplasm are similar to the parameters of the intranuclear movement of nuclear bodies like Cajal and PML (polymyelocytic leukemia) bodies (Platani *et al.*, 2002; Gőrich *et al.*, 2004), and also to the intranuclear dynamics of plasmid DNA localized inside the cell nucleus (Ondrej *et al.*, 2006). Because of the similar dynamic parameters of plasmids in both cytoplasm and nucleoplasm, the directional movement of plasmids inside the nucleus (Ondrej *et al.*, 2006), and the presence of nuclear actin in forms ranging from monomers to polymers (McDonald *et al.*, 2006), we suggest that the nuclear plasmids are also attached to actin polymers and could move along them for short distances.

Acknowledgements

REFERENCES

Anderson JL, Hope TJ (2005) *Gene Ther* **12**: 1667–1678.
Campbell EM, Hope TJ (2005) *Gene Ther* **12**: 1353–1359.
Coonrod A, Li FQ, Horwitz M (1997) *Gene Ther* **4**: 1313–1321.
Dauty E, Verkman AS (2005) *J Biol Chem* **280**: 7823–7828.
Gőrisch SM, Wachsmuth M, Ittrich C, Bacher CP, Rippe K, Lichter P (2004) *Proc Natl Acad Sci USA* **101**: 13221–13226.
Gruenheid S, Finlay BB (2003) *Nature* **422**: 775–781.
Johnson AL, Jurcisek JA (1999) *AAPS Pharmsci* 1, e6.
Kozubek M, Kozubek S, Lukášová E, Bártová E, Skalníková M, Matula P, Matula P, Jirsová P, Cafourková A, Koutná I (2001) *Cytometry* **45**: 1–12.
Kozubek M, Matula P, Matula P, Kozubek S (2004) *Microsc Res Tech* **64**: 164–175.
Lee GE, Murray JW, Wolkoff AW, Wilson DW (2006) *J Virol* **80**: 4264–4275.
Lukacs GL, Haggie P, Seksek O, Lecherdeur D, Freedman N, Verkman AS (2000) *J Biol Chem* **275**: 1625–1629.
McDonald D, Vodicka MA, Lucero G, Svitkina TM, Borisy GG, Emerman M, Hope TJ (2002) *J Cell Biol* **159**: 441–452.
McDonald D, Carrero G, Andrin Ch, de Vries G, Hendzel MJ (2006) *J Cell Biol* **172**: 541–552.
Ondrej V, Kozubek S, Lukasova E, Falk M, Matula Pa, Matula P, Kozubek M (2006) *Chrom Res* **14**: 505–514.
Platani M, Goldberg I, Lamond AI, Swedlow JR (2002) *Nat Cell Biol* **4**: 502–508.
Shav-Tal Y, Singer RH (2005) *J Cell Sci* **118**: 4077–4081.
Van Loo ND, Fortunati E, Ehlert E, Rabelink M, Grosveld F, Scholte BJ (2001) *J Virol* **75**: 961–970.
Vaughan EE, Dean DA (2006) *Mol Ther* **13**: 422–428.
Zabner J, Fasbender AJ, Moninger T, Poellinger KA, Welsh MJ (1995) *J Biol Chem* **270**: 18997–19007.
Zhou R, Geiger Ch, Dean DA (2004) *Expert Opin Drug Deliv* **1**: 127–140.